PRAMANA
— journal of
physics

Vol. 84, No. 2
February 2015
pp. 257–272

Synchronization enhancement via an oscillatory bath in a network of self-excited cells

B R NANA NBENDJO[1], H G ENJIEU KADJI[1,2] and HILDA A CERDEIRA[3,*]

[1]Laboratory of Modelling and Simulation in Engineering and Biomimetics and Prototypes, University of Yaoundé I, P.O. Box 812, Yaoundé, Cameroon
[2]Monell Chemical Senses Center, 3500 Market Street, Philadelphia, PA 19104, USA
[3]Instituto de Física Teórica, UNESP-Universidade Estadual Paulista, Rua Dr. Bento Teobaldo Ferraz 271, Bloco II, 01140-070 São Paulo, SP, Brazil
*Corresponding author. E-mail: cerdeira@ift.unesp.br

DOI: 10.1007/s12043-014-0895-2; ***e*Publication:** 5 February 2015

Abstract. The possibility of using a dynamic environment to achieve and optimize phase synchronization in a network of self-excited cells with free-end boundary conditions is addressed in this paper. The dynamic environment is an oscillatory bath coupled linearly to a network of four cells. The boundaries of the stable solutions of the dynamical states as well as the ranges of coupling parameters leading to stability and instability of synchronization are determined. Numerical simulations are used to check the accuracy and to complement the result obtained from analytical treatment. The robustness of synchronization strategy is tested using a local and global injection of Gaussian white noise in the network. The control gain parameter of the bath coupling can modulate the occurrence of synchronization in the network without prior requirement of direct coupling among all the cells. The process of synchronization obtained through local injection is independent of the node at which noise is injected into the system. As compared to local injection, the global injection scheme increases the range of noise amplitude for which synchronization occurs in the network.

Keywords. Synchronization; oscillatory bath; self-excited cells; noise injection; network.

PACS Nos 87.18.Tt; 87.19.Im; 87.19.In; 87.19.lc

1. Introduction

Complex systems are highly organized to allow efficient processing of information [1–5]. Such expeditious process is correlated not only to network's configurations but also to cells or oscillators embedded in them. A widespread property shared across the board by these networks and which is independent of cell's type is synchronization [6–11], which can arise although isolated cells may possess either periodic or chaotic oscillatory states.

In addition to synchronization, other possible outputs from networks of oscillators are: riddled basins [12], on–off intermittency [13], spatiotemporal chaos, standard and generalized correlated states etc. [14]. The benefits of synchronization do not lie only in those situations where it can be found or explained in nature, but also in possible technological applications such as communication engineering, biology, chemistry and so on [15–24].

In previous attempts to analytically investigate the boundaries of stability of synchronization dynamics in networks of oscillators in non-chaotic states, for the most part, the focus has been on nearest neighbours and long-range couplings [7,14,19,25–28]. However, the key question of reinforcement of the synchronization process in networks remains an interesting task to address. This paper aims to investigate synchronization enhancement via an oscillatory bath in a network of coupled oscillators. An important problem where the notion of bath coupling applies is the chemistry of the eyes [29,30]. The idea consists of using a bath as inhibitor or catalyser or as external force to increase the range of synchronization occurring in the network. There is evidence that the eyes play an important role as the circardian pacemaker that drives the rhythm of ocular melatonin synthesis and that the pacemakers can remain locked even in constant darkness. Although there is no direct connection between the eyes, they are both connected to the brain, through the pineal gland located in the epithalamus [29–33]. Another important situation where part of the brain imposes its rhythm into biological functions is the role that the suprachiasmatic nuclei (SCN) plays in the circadian rhythms [32,34,35]. Most studies look at the problem as how the network of neurotransmitters in the SCN produces the necessary frequencies to impose the circadian cycle in the operations of the living beings. In this paper we have a different perspective: using the neuronal networks in the SCN or the neurotransmitters in the pineal gland as baths. In this paper we propose to use oscillators with a time limit cycle as the pacemakers, coupled to an environmental bath, which will represent the brain, which in this case will be the means of interaction between the oscillators, without necessarily having a proper frequency to impose the catalyser between those systems.

Thus, we use the strategy of environmental bath to shed some light on the issue of synchronization enhancement in a network of oscillators. The outline of the paper is as follows: In §2, we introduce the physical model and present the problem statement. Section 3 deals with the stability boundaries of the synchronization process while §4 addresses the effects of locally and globally injected Gaussian white noise on the synchronization process. Finally, conclusions are given in §4.

2. System configuration and problem statement

For the sake of simplicity, we limit the number of oscillators embedded in the network. Thus, the device shown in figure 1 represents a network of five oscillators. We use as oscillators circuit consisting of a condenser C, an inductor L and nonlinear resistor NR, all connected. The first four oscillators (1, 2, 3 and 4) are coupled to their nearest neighbour through the identical inductance L_c, while the fifth oscillator is connected to each of the first four oscillators through a different inductance $L_{\kappa 5}$ ($1 \leq \kappa \leq 5$). The current flowing through the nonlinear resistor is generally a function of the voltage (e.g., $I_\kappa^{\mathrm{Osc}} = F(\nu_1 V_\kappa + \nu_2 V_\kappa^2 + \nu_3 V_\kappa^3 + \cdots + \nu_N V_\kappa^N)$, where ν_1, ν_2, ν_3, ..., ν_N are constants. Throughout

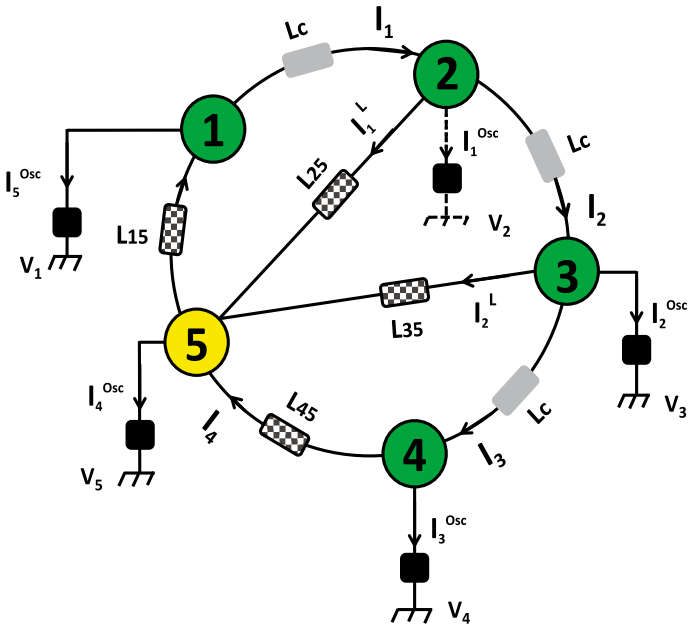

Figure 1. Network of four coupled self-excited cells (1, 2, 3, 4) in an oscillatory bath through the oscillator 5.

this paper, we assume the oscillators to be self-sustained/self-excited. This incentive is because the synchronization dynamics of complex systems composed of self-excited cells occurs in many fields such as in biology, physics and neuroscience. Here, each self-excited cell is modelled by a classical van der Pol oscillator (vdPol) (figure 2). Under such circumstances, the voltage–current equation of the NR [36] is defined as follows:

$$I_{\kappa}^{\mathrm{vdP}} = -a_1 V_{\kappa} + a_3 V_{\kappa}^3, \tag{1}$$

where a_1 and a_3 stand for positive constants. The NR, which incorporates a dissipative mechanism to damp oscillations that become too large and a source of energy to pump up those that become too small, can be realized by using a block consisting of two transistors [36]. In such situations, the device traces a particular path through phase space, and if a perturbation excites it out of its accustomed rhythm, it soon returns to its former path. Oscillators that have a standard waveform and amplitude to which they return after small

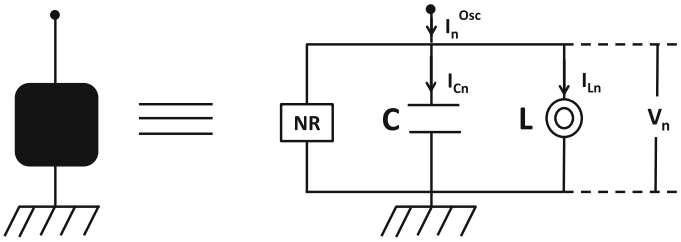

Figure 2. Electrical model of a self-excited oscillator.

perturbations are known as stable limit-cycle oscillators, which are self-sustained. In physiological expressions, the capacitor C represents a cellular membrane where ions are drained by a nonlinear resistance NR. The inductance L models the finite switching time of the ion channels in the membrane.

As shown in the Appendix, the model is described by the following second-order non-dimensional, nonlinear differential equations:

$$\begin{aligned}
\ddot{x}_1 - \mu(1-x_1^2)\dot{x}_1 + x_1 &= K(x_2 - x_1) + G(x_5 - x_1),\\
\ddot{x}_2 - \mu(1-x_2^2)\dot{x}_2 + x_2 &= K(x_3 - 2x_2 + x_1) + G(x_5 - x_2),\\
\ddot{x}_3 - \mu(1-x_3^2)\dot{x}_3 + x_3 &= K(x_4 - 2x_3 + x_2) + G(x_5 - x_3),\\
\ddot{x}_4 - \mu(1-x_4^2)\dot{x}_4 + x_4 &= K(x_3 - x_4) + G(x_5 - x_4),\\
\ddot{x}_5 - \mu(1-x_5^2)\dot{x}_5 + x_5 &= G(x_1 - x_5) + G(x_2 - x_5)\\
&\quad + G(x_3 - x_5) + G(x_4 - x_5),
\end{aligned} \tag{2}$$

where the overdot denotes the derivative with respect to time t. x_i represents the dimensionless electric current at the κth oscillator, μ is a positive coefficient denoting the nonlinear parameter, K is the coupling parameter and G is the control gain parameter of the system. The final state of the vdPol is purely sinusoidal for small values of μ, developing into quasisinusoidal and relaxation oscillations as μ increases [37,38].

3. Stability analysis of phase synchronization

3.1 *Analytical treatment*

The network under consideration is interesting only if its resulting dynamical state is stable. This requires all perturbed trajectories to return to the original limit cycle. It is then particularly important to develop criteria that guarantee the asymptotic stability of the synchronization process if applications are sought. Moreover, one can tolerate synchronization failure but not its instability because it could damage the system.

The linear stability analysis of the dynamical states can be performed by linearizing eqs (2) around the unperturbed limit cycle (or orbit) x_o according to the following equations:

$$\begin{aligned}
\ddot{\varepsilon}_1 - \mu(1-x_o^2)\dot{\varepsilon}_1 + (1 + 2\mu x_o\dot{x}_o)\varepsilon_1 &= K(\varepsilon_2 - \varepsilon_1) + G(\varepsilon_5 - \varepsilon_1),\\
\ddot{\varepsilon}_2 - \mu(1-x_o^2)\dot{\varepsilon}_2 + (1 + 2\mu x_o\dot{x}_o)\varepsilon_2 &= K(\varepsilon_3 - 2\varepsilon_2 + \varepsilon_1) + G(\varepsilon_5 - \varepsilon_2),\\
\ddot{\varepsilon}_3 - \mu(1-x_o^2)\dot{\varepsilon}_3 + (1 + 2\mu x_o\dot{x}_o)\varepsilon_3 &= K(\varepsilon_4 - 2\varepsilon_3 + \varepsilon_2) + G(\varepsilon_5 - \varepsilon_3),\\
\ddot{\varepsilon}_4 - \mu(1-x_o^2)\dot{\varepsilon}_4 + (1 + 2\mu x_o\dot{x}_o)\varepsilon_4 &= K(\varepsilon_3 - \varepsilon_4) + G(\varepsilon_5 - \varepsilon_4),\\
\ddot{\varepsilon}_5 - \mu(1-x_o^2)\dot{\varepsilon}_5 + (1 + 2\mu x_o\dot{x}_o)\varepsilon_5 &= G(\varepsilon_1 + \varepsilon_2 + \varepsilon_3 + \varepsilon_4 - 4\varepsilon_5),
\end{aligned} \tag{3}$$

where ε_κ $(1 \le \kappa \le 5)$ are the perturbations introduced. For small values of μ, the dynamics of each of the oscillator can be described in the first approximation by a pure sinusoidal trajectory of the form:

$$x_o = A\cos(\omega t - \phi), \tag{4}$$

where A, ω and ϕ are, respectively the amplitude, frequency and the phase of the unperturbed limit cycle. As reported in [39] dealing with the synchronization of two vdPols, such a first-order approximation gives a fairly good agreement between the analytical and numerical results. For $\mu = 0.1$, the values of A and ω are 2 and 0.999, respectively. Using the solution (4), the variational eqs (3) can be rewritten as follows:

$$\begin{aligned}
\ddot{\varepsilon}_1 &+ \left[\alpha + \frac{\mu A^2}{2\omega}\cos 2\tau\right]\dot{\varepsilon}_1 + \frac{1}{\omega^2}(\delta_1 - \mu A^2\omega \sin 2\tau)\varepsilon_1 = \frac{K}{\omega^2}\varepsilon_2 + \frac{G}{\omega^2}\varepsilon_5,\\
\ddot{\varepsilon}_2 &+ \left[\alpha + \frac{\mu A^2}{2\omega}\cos 2\tau\right]\dot{\varepsilon}_2 + \frac{1}{\omega^2}(\delta_2 - \mu A^2\omega \sin 2\tau)\varepsilon_2 = \frac{K}{\omega^2}\varepsilon_1 + \frac{K}{\omega^2}\varepsilon_3 + \frac{G}{\omega^2}\varepsilon_5,\\
\ddot{\varepsilon}_3 &+ \left[\alpha + \frac{\mu A^2}{2\omega}\cos 2\tau\right]\dot{\varepsilon}_3 + \frac{1}{\omega^2}(\delta_3 - \mu A^2\omega \sin 2\tau)\varepsilon_3 = \frac{K}{\omega^2}\varepsilon_2 + \frac{K}{\omega^2}\varepsilon_4 + \frac{G}{\omega^2}\varepsilon_5,\\
\ddot{\varepsilon}_4 &+ \left[\alpha + \frac{\mu A^2}{2\omega}\cos 2\tau\right]\dot{\varepsilon}_4 + \frac{1}{\omega^2}(\delta_4 - \mu A^2\omega \sin 2\tau)\varepsilon_4 = \frac{K}{\omega^2}\varepsilon_3 + \frac{G}{\omega^2}\varepsilon_5,\\
\ddot{\varepsilon}_5 &+ \left[\alpha + \frac{\mu A^2}{2\omega}\cos 2\tau\right]\dot{\varepsilon}_5 + \frac{1}{\omega^2}(\delta_5 - \mu A^2\omega \sin 2\tau)\varepsilon_5\\
&= \frac{G}{\omega^2}\varepsilon_1 + \frac{G}{\omega^2}\varepsilon_2 + \frac{G}{\omega^2}\varepsilon_3 + \frac{G}{\omega^2}\varepsilon_4, \qquad (5)
\end{aligned}$$

with

$$\alpha = \frac{\mu}{\omega}\left(\frac{A^2}{2} - 1\right), \quad \delta_1 = \delta_4 = \frac{1}{\omega^2}(1 + K + G),$$

$$\delta_2 = \delta_3 = \frac{1}{\omega^2}(1 + 2K + G), \quad \delta_5 = \frac{1}{\omega^2}(1 + 4G).$$

As assessing the stability of synchronized states around resonant states is difficult, our first approach is to investigate the stability analysis far from those states. Thus, the stability matrix of eq. (5) is block-diagonalized to determine the following eigenvalues λ_ν ($1 \leq \nu \leq 10$):

$$\lambda_1 = \frac{-1 - \sqrt{-399 - 400G + 400(\sqrt{2} - 2)K}}{20},$$

$$\lambda_2 = \frac{-1 + \sqrt{-399 - 400G + 400(\sqrt{2} - 2)K}}{20},$$

$$\lambda_3 = \frac{-1 - \sqrt{-399 - 400G - 400(\sqrt{2} + 2)K}}{20},$$

$$\lambda_4 = \frac{-1 + \sqrt{-399 - 400G - 400(\sqrt{2} + 2)K}}{20},$$

$$\lambda_5 = \frac{-1 - \sqrt{-399 - 400G - 800K}}{20},$$

$$\lambda_6 = \frac{-1+\sqrt{-399-400G-800K}}{20},$$
$$\lambda_7 = \frac{-1-\sqrt{-399-2000G}}{20},$$
$$\lambda_8 = \frac{-1+\sqrt{-399-2000G}}{20},$$
$$\lambda_9 = \frac{-1-j\sqrt{399}}{20},$$
$$\lambda_{10} = \frac{-1+j\sqrt{399}}{20}. \tag{6}$$

Complete stability occurs only if all eigenvalues possess negative real parts. Accordingly, the stability of the synchronization process is guaranteed if the following criteria are fulfilled:

$$G \in (-0.2, +\infty) \tag{7}$$
$$K \in \left(\frac{-1-G}{2+\sqrt{2}}, +\infty\right). \tag{8}$$

If conditions (7) and (8) are not simultaneously fulfilled, the synchronization will be unstable and therefore, as t increases, $\varepsilon(t)$ will never go to zero but will possess a bounded oscillatory behaviour or goes to infinity.

3.2 *Numerical analysis*

Numerical simulations of eqs (2) are carried out to determine the accuracy and to complement the analytical results obtained. The numerical simulation uses the fourth-order Runge–Kutta algorithm with a time step $\Delta t = 0.01$ and the following initial conditions $(x_1(0); \dot{x}_1(0)) = (1.0; 1.0)$, $(x_2(0); \dot{x}_2(0)) = (1.5; 1.5)$, $(x_3(0); \dot{x}_3(0)) = (2.0; 2.0)$, $(x_4(0); \dot{x}_4(0)) = (2.5; 2.5)$ and $(x_5(0); \dot{x}_5(0)) = (2.5; 2)$. Synchronization between two oscillators u and v is defined with a criterion that the distance of the phase trajectories is

$$d_{uv} = |u - v| < h, \tag{9}$$

where $h = 10^{-4}$ represents the accuracy. The synchronization among all four oscillators is effective if the total separation (TS) of all oscillator pairs is smaller than the accuracy, i.e.,

$$\mathrm{TS} = \sum_{\mathrm{pairs}(uv)} d_{uv} < h. \tag{10}$$

For higher precision, computational time has been extended to 10^4.

In the absence of an oscillatory bath ($G = 0$ and $(x_5(0); \dot{x}_5(0)) = (0; 0)$), only the first four oscillators are considered. In such a condition, the network is fully synchronized for $K \in [-0.2363, -0.0017] \cup [0.037, +\infty)$ as previously reported [28]. But once an oscillatory bath is taken into account ($G \neq 0$) as part of the network through

the fifth oscillator, the synchronization domains expand beyond the boundaries obtained in the absence of a bath. Moreover, the network can be fully synchronized even if the first oscillators are not initially coupled (i.e., $K = 0$). These findings demonstrate the enhancement effect that the oscillatory bath has in the synchronization of the oscillators. For instance, when the bath strength $G = 0.3$, the network displays a complete synchronization for $K \in [-0.35, -0.110] \cup [-0.076, 0.105] \cup [0.234, +\infty)$ while for $K \in [-0.109, -0.077] \cup [0.106, 0.233]$, no synchronization occurs in the system. As G increases (e.g., $G = 0.6$), all the oscillators in the network are synchronized for $K \in [-0.35, -0.203] \cup [-0.169, 0.266] \cup [0.403, +\infty)$ while instability occurs for $K \in [-0.202, -0.170] \cup [0.267, 0.402]$. The process of synchronization is considered unstable if, as time increases, TS never goes to zero, but shows bounded oscillations or goes to infinity. Time histories of TS showing synchronization and instability of oscillations for three sets of (K, G) are plotted in figure 3. In order to determine a broader picture of the system's behaviour for wider ranges of coupling parameters (K, G), a stability chart summarizing domains of synchronized states which occur in the network are plotted in figure 4. Besides, as not all values of K and G are able to lead either to stability or instability of the processes, it becomes interesting to define their admissible values for the network under consideration. Thus, critical boundaries of the coupling parameters K and G are provided in the plane (G, K) as shown in figure 5, where the set

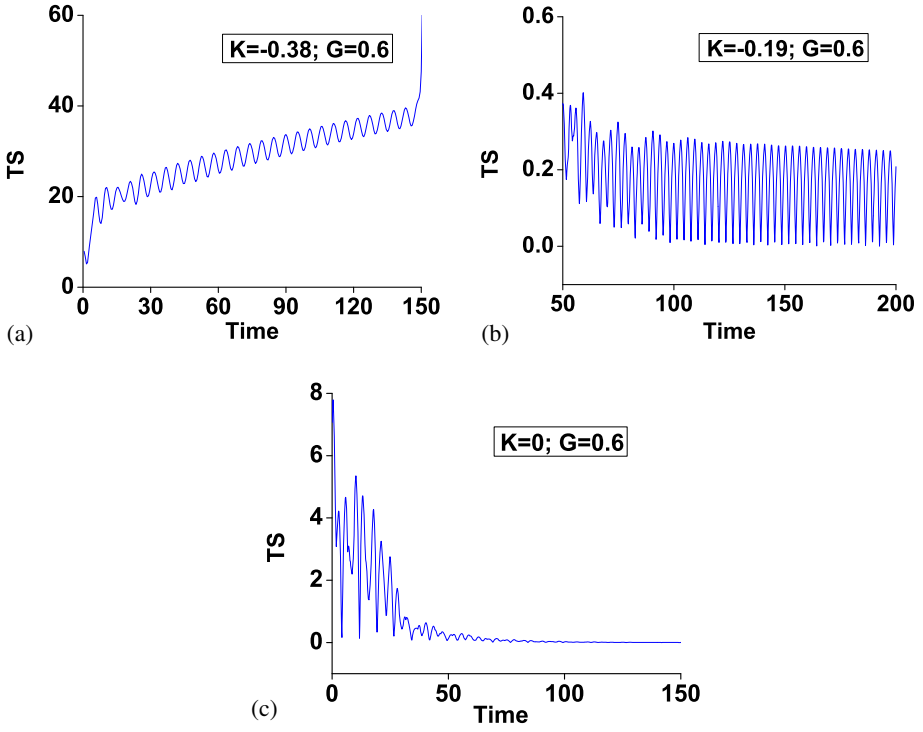

Figure 3. Time histories of TS displaying synchronized states: (**a**) and (**b**) show instability of the process while (**c**) shows full synchronization.

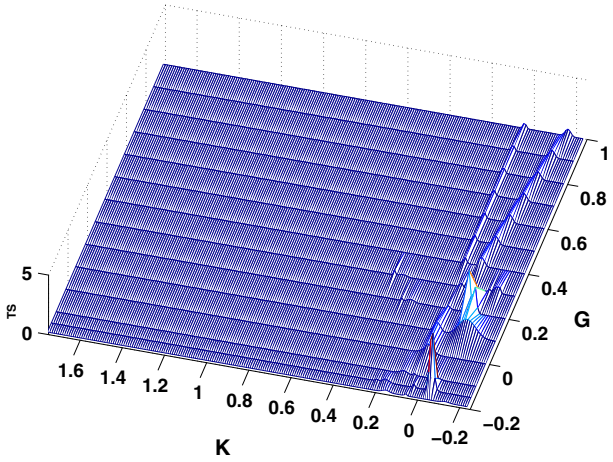

Figure 4. Chart displaying all dynamical states of the network and their stability boundaries. When any set of (K, G) leads to TS $= 0$, the synchronization is fully stable. But when TS $\neq 0$, the process of synchronization is unstable for the corresponding sets of (K, G). The regions of instability are mostly found for $K > -0.1$.

of coupling parameters leading to either bounded or unbounded oscillatory states, or to full synchronization is above the curve while the region below the curve corresponds to sets of forbidden values of the coupling parameters.

3.3 *Influence of an injected noise on the synchronization process*

Here, we consider both the local and global injection schemes. The local injection technique consists of a unidirectional coupling between the external command oscillator and a

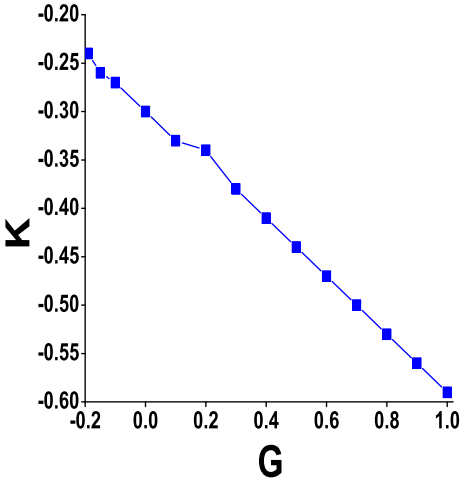

Figure 5. Critical boundaries of the coupling parameters G and K. For (G, K) considered above the curve, the process of synchronization is either stable or unstable. The region below the curve defines non-admissible values of (G, K) for the system.

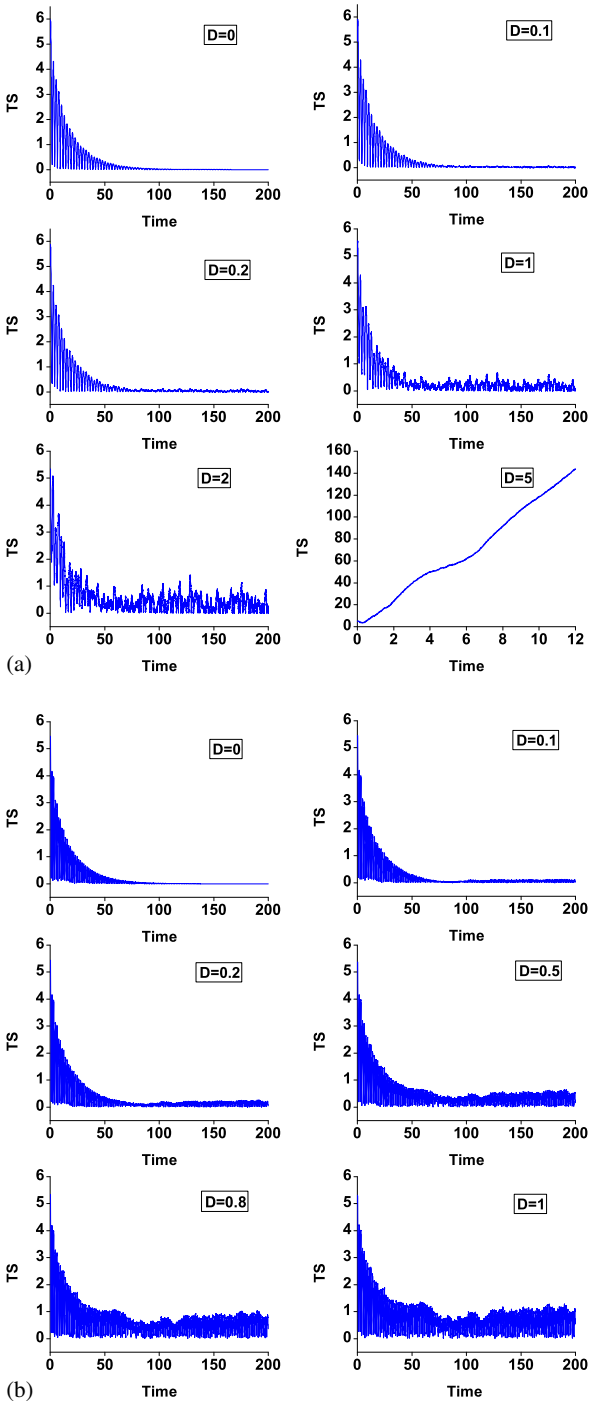

(a)

(b)

Figure 6. Effects of the white noise on the synchronization process. **(a)** $K = 0$, $G = 0.6$; **(b)** $K = 5$, $G = 0.3$.

fixed representative of the nonlinear coupled system [40]. Such a technique is interesting and widely used in many scientific areas, ranging from physics, engineering and biology [26,27,41–43]. One example is electrophysiological experiments for drug delivery at a specific site of a neuron/neuronal network [44]. Also, in order to investigate propagation of somatic or dendritic action potential at a single cell level, this technique is required during patch clamp experiments for current injection (current-clamp mode) in the cell body or dendrite [45,46]. In this way, the dynamics of a neuron/neuronal network can be monitored by a locally injected current in electrical and/or synaptic coupling among cells [47,48]. In our model, Gaussian white noise is locally injected in the first cell within the array to monitor the stability boundaries of synchronization patterns that occur. In such a condition, the state variables of the network are described by the following set of second-order non-dimensional, nonlinear differential equations:

$$\begin{aligned}
\ddot{x}_1 - \mu(1-x_1^2)\dot{x}_1 + x_1 &= K(x_2 - x_1) + G(x_5 - x_1) + \xi(t),\\
\ddot{x}_2 - \mu(1-x_2^2)\dot{x}_2 + x_2 &= K(x_3 - 2x_2 + x_1) + G(x_5 - x_2),\\
\ddot{x}_3 - \mu(1-x_3^2)\dot{x}_3 + x_3 &= K(x_4 - 2x_3 + x_2) + G(x_5 - x_3),
\end{aligned}$$

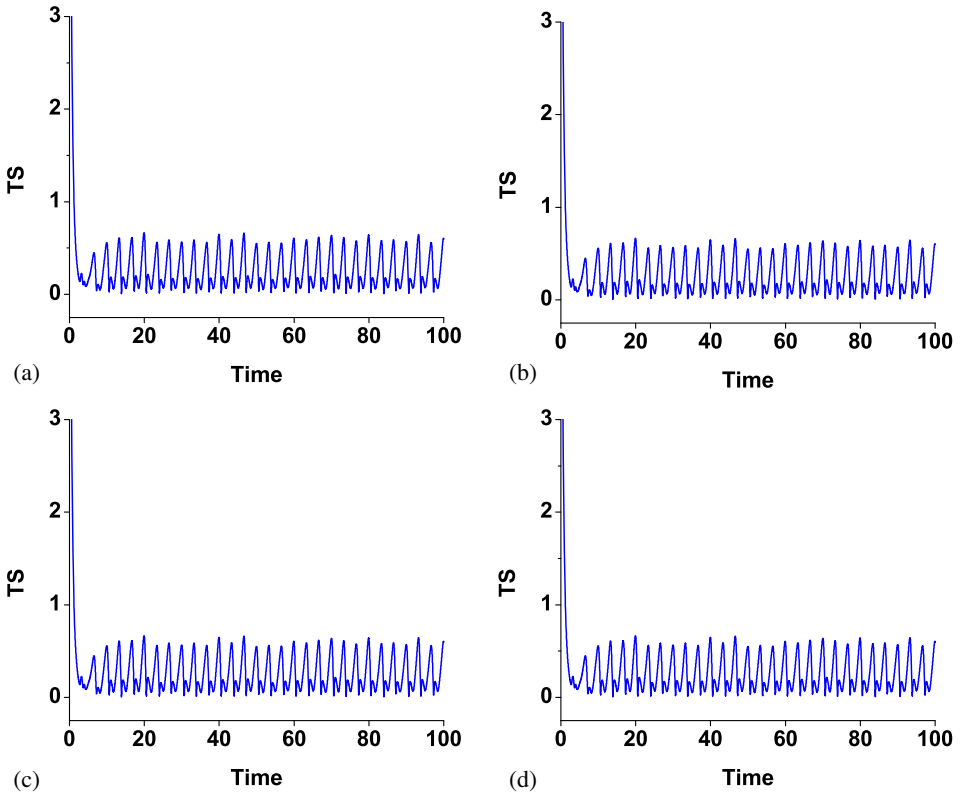

Figure 7. Effect of white noise injection on the synchronization process when locally injected in different oscillators for $K = 5$, $G = 0.3$, $D = 0.5$. **(a)** In oscillator 1; **(b)** in oscillator 2; **(c)** in oscillator 3; **(d)** in oscillator 4.

$$\ddot{x}_4 - \mu(1 - x_4^2)\dot{x}_4 + x_4 = K(x_3 - x_4) + G(x_5 - x_4),$$
$$\ddot{x}_5 - \mu(1 - x_5^2)\dot{x}_5 + x_5 = G(x_1 - x_5) + G(x_2 - x_5) + G(x_3 - x_5) + G(x_4 - x_5), \quad (11)$$

where $\xi(t)$ plays the role of the command signal and also stands for the dynamics of the external oscillator. The stochastic term $\xi(t)$ is a Gaussian white noise of zero mean (i.e., $\langle\xi(t)\rangle = 0$ and $\langle\xi(t)\xi(t')\rangle = 0$) and correlation $\langle\xi(t)\xi(t')\rangle = 2D\delta(t - t')$ with D being the intensity of the noise. Here, the effects of noise on the synchronization process is investigated at two different scales: locally and globally. In the case of a locally injected white noise through the oscillator 1 as defined earlier, it is found very interesting that when all oscillators are only coupled via an oscillatory bath ($G \neq 0$, $K = 0$), the full synchronization can still occur in the network as shown in figure 6a. When the coupling strength among the oscillators 1, 2, 3 and 4 are not null, the full synchronization can

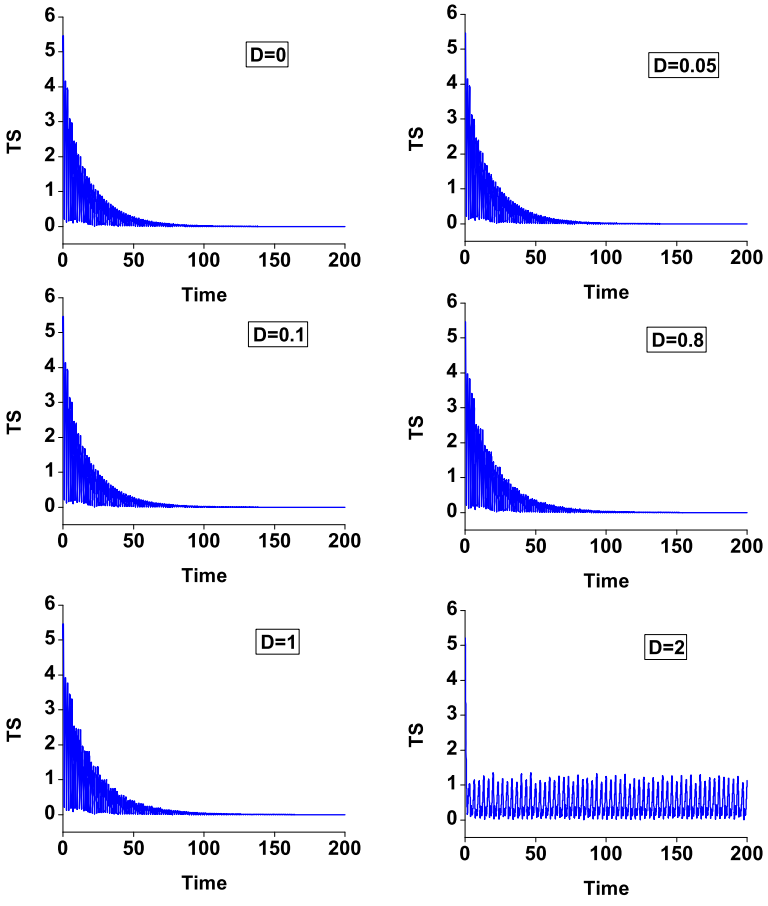

Figure 8. Effect of white noise injection on the synchronization process when globally injected in the oscillators 1, 2, 3 and 4. $K = 5$, $G = 0.3$.

still be found in the network. Nevertheless, as the amplitude of noise becomes bigger, the robustness of synchronization via an environmental bath is disrupted, leading in some cases (e.g., $D = 1, 5$) to full instability of the process. The location of noise injection in the network has no influence on the network output as reported in figure 7.

In physiological conditions where multiple connections exist among cells, each of them receive noisy input. In such conditions, the noise is not localized but spatially extended through the whole system [49]. Additionally, the injection of common random noises has been proven efficient in synchronizing chaotic systems [50]. In order to mimic the effects of spatially extended noise on the synchronization dynamics in the system under consideration, a zero-mean Gaussian white noise is globally injected in all the four oscillators. Under these circumstances, the network is now described by the equations below:

$$\begin{aligned}
\ddot{x}_1 - \mu(1-x_1^2)\dot{x}_1 + x_1 &= K(x_2 - x_1) + G(x_5 - x_1) + \xi(t),\\
\ddot{x}_2 - \mu(1-x_2^2)\dot{x}_2 + x_2 &= K(x_3 - 2x_2 + x_1) + G(x_5 - x_2) + \xi(t),\\
\ddot{x}_3 - \mu(1-x_3^2)\dot{x}_3 + x_3 &= K(x_4 - 2x_3 + x_2) + G(x_5 - x_3) + \xi(t),\\
\ddot{x}_4 - \mu(1-x_4^2)\dot{x}_4 + x_4 &= K(x_3 - x_4) + G(x_5 - x_4) + \xi(t),\\
\ddot{x}_5 - \mu(1-x_5^2)\dot{x}_5 + x_5 &= G(x_1 - x_5) + G(x_2 - x_5)\\
&\quad + G(x_3 - x_5) + G(x_4 - x_5). \qquad (12)
\end{aligned}$$

The results of numerical simulation in this case reveal that compared to local injection, global injection of noise makes the process of synchronization more robust for some range of D. This robustness of global injection of noise can be visualized by comparing the plots shown in figure 6b and figure 8.

4. Conclusion

In this paper, we have examined the possibility of using an external environment to optimize the process of synchronization in a network of self-excited cells. Each cells within the network was modelled as a van der Pol oscillator whose phase depends on initial conditions. The properties of eigenvalues have allowed to analytically predict stability boundaries of the coupling parameters K and G for which the phase synchronization is successful. These boundaries have been validated using numerical simulations. The critical frontiers of both coupling parameters for which all possible dynamical states exist have been provided. A key finding here has been to use an external dynamic environment to enhance the process of synchronization in the network of self-excited cells. Moreover, in a bath environment, synchronization can be achieved without prior requirement of direct coupling (i.e., $K = 0$) among self-excited cells which are embedded in a network with free-end boundary conditions. The influence of a stochastic signal in the form of Gaussian white noise locally and globally injected in the network has been investigated. In both cases, the robustness of synchronization in the presence of a bath was stronger for higher noise intensity in global injection. But as for the local injection, the test has been successful for lower noise intensity. Although this model specifically focusses on self-excited cells, this study can be extended to different types of oscillators.

Acknowledgements

Part of this work was completed during a research visit of Dr Nana Nbendjo at the Institute of Theoretical Physics-State University of São Paulo in Brazil. He is grateful to Brazilian Government (CNPq) for financial support within the project CNPq/PROAFRICA 490265/2010-3.

Appendix

The Kirchhoff's laws for each of the oscillator are as follows:

Oscillator 1:

$$V_1 - V_2 = L_C \frac{\mathrm{d}I_1}{\mathrm{d}\tau}$$
$$V_5 - V_1 = L_{15} \frac{\mathrm{d}I_5}{\mathrm{d}\tau}$$
$$I_5 = I_5^{\mathrm{Osc}} + I_1.$$

Oscillator 2:

$$V_2 - V_3 = L_C \frac{\mathrm{d}I_2}{\mathrm{d}\tau}$$
$$V_2 - V_5 = L_{25} \frac{\mathrm{d}I_1^L}{\mathrm{d}\tau}$$
$$I_1 = I_1^L + I_1^{\mathrm{Osc}} + I_2.$$

Oscillator 3:

$$V_3 - V_4 = L_C \frac{\mathrm{d}I_3}{\mathrm{d}\tau}$$
$$V_3 - V_5 = L_{35} \frac{\mathrm{d}I_2^L}{\mathrm{d}\tau}$$
$$I_2 = I_3 + I_2^L + I_2^{\mathrm{Osc}}.$$

Oscillator 4:

$$V_3 - V_4 = L_C \frac{\mathrm{d}I_3}{\mathrm{d}\tau}$$
$$V_4 - V_5 = L_{45} \frac{\mathrm{d}I_4}{\mathrm{d}\tau}$$
$$I_3 = I_4 + I_3^{\mathrm{Osc}}.$$

Oscillator 5:

$$V_4 - V_5 = L_{45}\frac{\mathrm{d}I_4}{\mathrm{d}\tau}$$

$$V_5 - V_1 = L_{15}\frac{\mathrm{d}I_5}{\mathrm{d}\tau}$$

$$V_2 - V_5 = L_{25}\frac{\mathrm{d}I_1^L}{\mathrm{d}\tau}$$

$$V_3 - V_5 = L_{35}\frac{\mathrm{d}I_2^L}{\mathrm{d}\tau}$$

$$I_4 = I_5 + I_4^{\mathrm{Osc}} - I_1^L - I_2^L.$$

From the above equations, the dynamics of the network in the case of vdPol oscillators is described by the following equations:

$$\frac{\mathrm{d}^2V_1}{\mathrm{d}\tau} - \frac{a_1}{C}\left(1-3\frac{a_3}{a_1}V_1^2\right)\frac{\mathrm{d}V_1}{\mathrm{d}\tau}+\frac{1}{LC}V_1=\frac{1}{L_CC}(V_2-V_1)+\frac{1}{L_{15}C}(V_5-V_1),$$

$$\frac{\mathrm{d}^2V_2}{\mathrm{d}\tau} - \frac{a_1}{C}\left(1-3\frac{a_3}{a_1}V_2^2\right)\frac{\mathrm{d}V_2}{\mathrm{d}\tau}+\frac{1}{LC}V_2 = \frac{1}{L_CC}(V_1-2V_2+V_3)+\frac{1}{L_{25}C}(V_5-V_2),$$

$$\frac{\mathrm{d}^2V_3}{\mathrm{d}\tau} - \frac{a_1}{C}\left(1-3\frac{a_3}{a_1}V_3^2\right)\frac{\mathrm{d}V_3}{\mathrm{d}\tau}+\frac{1}{LC}V_3 = \frac{1}{L_CC}(V_2-2V_3+V_4)+\frac{1}{L_{35}C}(V_5-V_3),$$

$$\frac{\mathrm{d}^2V_4}{\mathrm{d}\tau} - \frac{a_1}{C}\left(1-3\frac{a_3}{a_1}V_4^2\right)\frac{\mathrm{d}V_4}{\mathrm{d}\tau}+\frac{1}{LC}V_4=\frac{1}{L_CC}(V_3-V_4)+\frac{1}{L_{45}C}(V_5-V_4),$$

$$\frac{\mathrm{d}^2V_5}{\mathrm{d}\tau} - \frac{a_1}{C}\left(1-3\frac{a_3}{a_1}V_5^2\right)\frac{\mathrm{d}V_5}{\mathrm{d}\tau}+\frac{1}{LC}V_5 = \frac{1}{L_{15}C}(V_1-V_5)+\frac{1}{L_{25}C}(V_2-V_5)+\frac{1}{L_{35}C}(V_3-V_5)+\frac{1}{L_{45}C}(V_4-V_5),$$

where

$$\mu = a_1\sqrt{\frac{L}{C}}, \quad \omega^2 = \frac{1}{LC}, \quad V_\kappa = \sqrt{\frac{a_1}{3a_3}}x_\kappa, \quad t = \omega\tau,$$

$$K = \frac{L}{L_C}, \quad G_i = \frac{L}{L_{i5}}, \quad 1 \le i \le 5, \quad L_{15} = L_{25} = L_{35} = L_{45}.$$

References

[1] D J Watts and S H Strogatz, *Nature* **394**, 440 (1998)
[2] S Song, P J Sjostrom, M Reigl, S Nelson and D B Chklovskii, *PLoS Biol.* **3**, 0507 (2005)
[3] L Donetti, P I Hurtado and M A Muñoz, *Phys. Rev. Lett.* **95**, 188701 (2005)
[4] B Wang, T Zhou, Z L Xiu and B J Kim, *Eur. Phys. J. B* **60**, 89 (2007)
[5] A A Selivanov, J Lehnert, T Dahms, P Hovel, A L Fradkov and E Scholl, *Phys. Rev. E* **85**, 016201 (2012)
[6] Y Xie, Y Gong, Y Hao and X Ma, *Biophys. Chem.* **146**, 126 (2009)
[7] F Sorrentino, *New J. Phys.* **14**, 033035 (2012)
[8] I K Rhee, J Lee, J Kim, E Serpedin and Y C Wu, *Sensors* **9**, 56 (2009)
[9] L Zhao, I I B Beverlin, T Netoff and D Q Nykamp, *Frontiers Comput. Neurosci.* **5**, 1 (2011)
[10] K Lehnertz, S Bialonski, M T Horstmann, D Krung, A Rothkegel, M Staniek and T Wagner, *J. Neurosci. Meth.* **183**, 42 (2009)
[11] H G Enjieu Kadji, J B Chabi Orou and P Woafo, *Commun. Nonlinear Sci. Numer. Simul.* **13**, 1361 (2007)
[12] P Ashwin, *Lect. Notes Phys.* **671**, 181 (2005)
[13] A M Dos Santos, S Lopez and R L Viana, *Math. Probl. Eng.* **2009**, 610574 (2009)
[14] Y Chembo Kouomou and P Woafo, *Phys. Rev. E* **67**, 046205 (2003)
[15] Z Zheng, X Feng, B Ao and M C Cross, *Europhys. Lett.* **87**, 50006 (2005)
[16] J Zhou, H B Huang, G X Qi, P Yang and X Xie, *Phys. Lett. A* **335**, 191 (2005)
[17] N Komin, A C Murza, E Hernández García and R Toral, *Interface Focus* **1**, 167 (2011)
[18] L J Kocarev, K S Halle, K Eckert, U Parlitz and L O Chua, *Int. J. Bifurcat. Chaos* **2**, 709 (1992)
[19] Y Kuramoto, *Chemical oscillations, waves and turbulence* (Springer-Verlag, New York, 1980)
[20] F Song, M He, M I Faley, L Fang and A M Klushin, *J. Appl. Phys.* **108**, 063903 (2010)
[21] J Benford, H Sze, W Woo, R R Smith and B Harteneck, *Phys. Rev. Lett.* **62**, 969 (1989)
[22] A Ishaaya, V Eckouse, L Shimshi, N Davidson and A Friesem, *Opt. Express* **13**, 2722 (2005)
[23] S Peles, J L Rogers and K Wiesenfeld, *Phys. Rev. E* **73**, 026212 (2006)
[24] R Yamapi, H G Enjieu Kadji and G Filatrella, *Nonlinear Dynam.* **61**, 275 (2010)
[25] H G Enjieu Kadji, J B Chabi Orou and P Woafo, *Chaos* **17**, 033109 (2007)
[26] C Lia, H Xu, X Liao and J Yu, *Physica A* **395**, 359 (2004)
[27] H F El-Nashar, Y Zhang and H A Cerdeira, *Chaos* **13**, 1216 (2003)
[28] P Woafo and H G Enjieu Kadji, *Phys. Rev. E* **69**, 046206 (2004)
[29] E Camacho, R Rand and H Howland, *Int. J. Solids Struct.* **41**, 2133 (2004)
[30] C T Steele, B D Zivkovic, T Siopes and H Underwood, *Am. J. Physiol. Regul. Integr. Comp. Physiol.* **284**, 208 (2003)
[31] R J Thresher, M H Vitaterna, Y Miyamoto, A Kazantsev, D S Hsu, C Petit, C P Selby, L Dawut, O Smithies, J S Takahashi and A Sancar, *Science* **282**, 5393 (1998)
[32] S Hattar, H W Liao, M Takao, D M Berson and K W Yau, *Science* **295**, 5557 (2002)
[33] M K Manglapus, P M Iuvone, H Underwood, M E Pierce and R B Barlow, *J. Neurosci.* **19**, 4132 (1999)
[34] N P A Bos and M Mirmiran, *Brain Res.* **511**, 1 (1990)
[35] M U Gillete and S A Tischkau, *Recent Prog. Hormone Res.* **54**, 33 (1999)
[36] B Nana and P Woafo, *Phys. Rev. E* **74**, 046213 (2006)
[37] A H Nayfeh and D T Mook, *Nonlinear oscillations* (Wiley, New York, 1979)
[38] C Hayashi, *Nonlinear oscillations in physical systems* (McGraw-Hill, New York, 1964)

[39] H G Enjieu Kadji, R Yamapi and J B Chabi Orou, *Chaos* **17**, 033113 (2007)
[40] H Gang, X Jinghua, G Jihua, L Xiangming, Y Yugui and B Hu, *Phys. Rev. E* **62**, R3034 (2000)
[41] J D Menietti, O Santolik, A M Rymer, G B Hospodarsky, A M Persoon, D A Gurnett, J Coates and D T Young, *J. Geophys. Res.* **113**, A05213 (2008)
[42] Y Takiguchi, Y Liu and J Ohtsubo, *Opt. Lett.* **23**, 1369 (1998)
[43] J R Lieberman, A Daluiski and T A Einhorn, *J. Bone. Joint. Surg. Am.* **84**, 1032 (2002)
[44] M Ellies, R Laskawi, G Tormahlen and W Gotz, *J. Oral Maxillofac. Surg.* **58**, 1251 (2000)
[45] S C Jung and D A Hoffman, *PLoS One* **4** e6549 1–14 (2009)
[46] N Keren, D Bar-Yehuda and A Korngreen, *J. Physiol.* **587**, 1413 (2009)
[47] M Galarreta and S Hestrin, *Nature* **402**, 72 (1999)
[48] G Silberberg and H Markram, *Neuron* **53**, 735 (2007)
[49] A S Landsman, E Neftci and D R Muir, *New J. Phys.* **14**, 1 (2012)
[50] R Toral, C R Mirasso, E Hernandez-Garcia and O Piro, *Chaos* **11**, 665 (2001)